Leading-Edge Vortex Structure for Flow over the Gliding Butterfly

Y. Hu, and J. J. Wang *
Beijing University of Aeronautics and Astronautics, Beijing 100191, People's Republic of China

ABSTRACT

The dye visualization experiment shows that a leading edge dual vortex structure exists on the suction surface of the simplified butterfly model of *Papilio ulysses* at α =8°, 10°, and 12°, respectively. Furthermore, the results of Particle Image Velocimetry (PIV) measurements indicate that the axial velocity of the primary (outer) leading-edge vortex core reaches the lower extreme value while the transition from a "wake-like" to a "jet-like" axial velocity profile occurs. This work will be contributed to the development of bionic butterfly-like MAVs.

1 INTRODUCTION

Recently, the development in micro technology accelerated the research on Micro-Air-Vehicles (MAVs), and flapping-wing MAVs in particular have attracted considerable attentions. The investigation on the flapping-wing locomotion has demonstrated that a small-sized flying insect not only generates sufficient lift to sustain its body aloft but also could control the flight with great precision [1], [2]. Insect flapping-wing flights can be sorted into two forms: high flapping frequency flights epitomized by the insects with small-scale wingspans such as drosophilae and bees, and low flapping frequency flights with large-scale wingspans such as butterflies and hawk moths. It is well known that a butterfly flies with high efficiency by combining flapping and gliding motions. Based on the observation of its flight gestures, researchers have obtained a lot of locomotion parameters in the last century [3]–[5].

In order to explain the high lift generation mechanism of butterfly flights, Srygley and Thomas [6] investigated the flow structures around a free flying red admiral butterfly in a wind tunnel by smoke-wire flow visualizations. The results indicated that some aerodynamic mechanisms including wake capture, two different types of leading-edge vortex, active and inactive upstrokes are applied to provide more lift in successive strokes when the red admiral butterfly takes off, maneuvers, and lands, whereas these mechanisms are avoided in a steady forward flight. Kei et al. [7] calculated the aerodynamic force of the butterfly which was considered as a rigid multi-body system by Lagrangian method. Meanwhile, they also measured the aerodynamic force by a micro load cell to substantiate the validity of the mathematical model.

Up to now, the aerodynamic characteristics and the flow structures of butterflies have not been attached such importance to as their flight gestures. However, the gliding motions which do not occur in the small-scale insect flights are featured profoundly in butterfly flights, even more so than the flapping motions. In fact, the flow structures of the gliding motion are the primary aerodynamic mechanisms for migratory butterflies. Hence, research on the gliding flights of migratory butterflies can hopefully shed some light on the flight mechanism of large-scale flying insects. Hu et al. [8] used hydrogen bubble visualizations to observe the flow structures over a simplified model of *Papilio ulysses*(one species of migratory butterflies) and present the variations of these flow structures with angle of attack in detail. A new type of leading-edge vortices similar to an inverse Chinese character '八' was observed in the experiment (see Figure 1), which might have provided high lift for the butterfly to keep the body gravity in a gliding flight. Based on these observations, further efforts were made to explore the effect of the butterfly wing shape on the flow structures, and later led to the discovery that the leading edge radian can affect the shape and the strength of leading-edge vortices [9]. The oil flow visualizations and the unsteady force measurements were even carried out by Hu et al. [10] in a wind tunnel to clarify the relationships between the flow structures and the aerodynamic characteristics of the butterfly models.

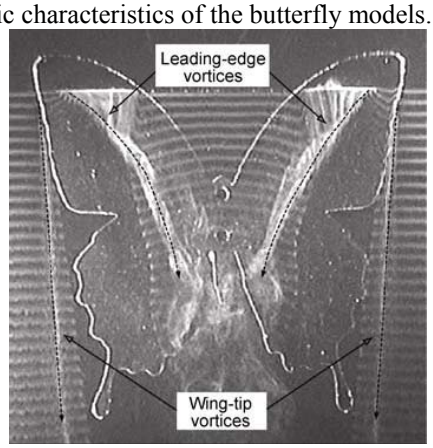

Figure 1: leading-edge vortices of a gliding butterfly (*Papilio ulysses*) at α =8° [8]

Although the hydrogen bubble visualizations [8] showed some flow structures on the suction surface of the butterfly model, the flow inside the leading-edge vortices was not observed in detail. This paper is focused on the leading-edge vortex structure of *Papilio ulysses* in a gliding flight. Dye visualizations and Particle Image Velocimetry (PIV) measurements for the simplified butterfly model are performed in a water tunnel. A new leading-edge vortex structure, i.e. the dual vortex structure, is observed in the dye visualization experiment. The axial velocity of the primary (outer) vortex core and its turbulence intensity on a plane through the primary leading-edge vortex core are considered in the PIV measurement. It is hoped that the present work will give more insight into the flight mechanism of the gliding butterfly.

Email address: jjwang@buaa.edu.cn

2 EXPERIMENTAL SETUP

The experiments have been conducted in a low speed recirculation water tunnel in Beijing University of Aeronautics and Astronautics. The working section of the water tunnel is 0.6m wide, 0.6m deep and 4.0m long. The free stream velocity can be adjusted in the range of 0~15.0cm/s automatically. The turbulence intensity of the free stream velocity is less than 0.8%.

In the present research, the simplified model of *Papilio ulysses* was tested which was the same as the model in Reference [8]. As shown in Figure 2, the model had a maximum chord length of *c*=200.0mm and a maximum span length of L=200.0mm, coincidentally. The free stream velocity was fixed at U=6.0cm/s in the experiments and the Reynolds number was Re=1.2×10^4 based on the maximum chord length of the model, which was close to the Reynolds number of an actual butterfly. The model was supported horizontally from the bottom in the working section and the support influence was not considered. The experimental angle of attack was varied from $\alpha = 4°$ to α =20° with a step of 2º and the angle of sideslip β was zero.

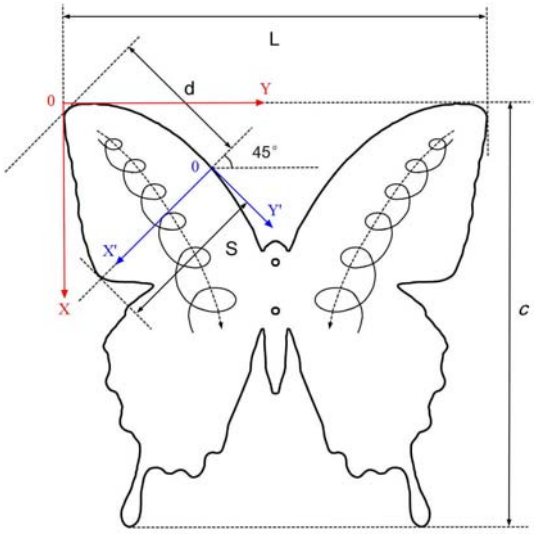

Figure 2: sketch of simplified *Papilio ulysses*
(Besides the butterfly model, the sketch contains the leading-edge vortices and two rectangular coordinate systems for dye visualizations and PIV measurements)

Flow visualizations were carried out by means of a mixed dye of Fluorescein Sodium and red ink injected into the flow near the leading edge via a long red copper tube with an inside diameter of $\phi_{\text{in}} = 0.3$mm and an outside diameter of ϕ_{out}= 0.5mm. The dye flow rate was controlled by a valve in the gravity feed line, which jointed the red copper tube and the bottle which contained the mixed dye. Moreover, the sectional flow structures were obtained by the laser sheet cutting the leading-edge vortex. The flow structures visualized by the dye were recorded by a CCD camera and image collection system. The two-dimensional Particle Image Velocimetry (PIV) measurements were performed on a plane through the primary leading-edge vortex core. Seeding hollow glass particles with a mean diameter of 5μm and a density of 1.05g/mm^3 were illuminated by a continuous laser sheet with a thickness of about 1mm and energy output of 1.5W. A high-speed CCD camera (640×480 pixels) captured a PIV interrogation plane of 80mm×60mm with a sampling frequency of 100Hz and duration of 50s. A commercial PIV software (MircroVec) was applied to analyze PIV images, and data post-processing was done by Tecplot and Matlab.

3 EXPERIMENTAL RESULT AND DISCUSSION

3.1 Dual Vortex Structure

In the flow visualization experiment, the mixed dye injected into the flow near the leading edge is involved into the leading-edge vortex core, and then the leading-edge vortex structure is visualized. When the dye is injected at a correct position in some special angles of attack, a leading edge dual vortex structure could be revealed on the suction surface of the butterfly model (see Figures 4-6) which is similar to the dual vortex structure of delta wings[11] –[13]. Because the model and the flow structures are symmetric, the imaging region is fixed on the left forewing in both the dye visualizations and the PIV measurements. In order to illustrate the spatial position and the size of the leading-edge vortex structure, two rectangular coordinate systems are defined on the left forewing of the butterfly model as shown in Figure 2. Top view is the projection of half a leading-edge vortex structure on the X-Y coordinate plane which is located on the left forewing surface of the model. X and Y axes are tangential to the left and the front edges of the model, respectively. The axis directions and the origin are shown in Figure 2(the red coordinate system), and the axis coordinates are non-dimensionalized by the wingspan length L. The sectional plane of a leading-edge vortex structure is on the X'-Z' coordinate plane (Z' axis is perpendicular to the wing surface and the direction accords to the right-hand rule). The distance from the sectional plane to the left extreme point of the model is d=70.0mm, and the length of the intersection line between the sectional plane and the model wing is S=72.0mm. In X'-Y' coordinate system (the blue coordinate system in Figure 2), the origin is the intersection point of the sectional plane and the left leading edge, and the axis coordinates are normalized by the intersection line length S.

Figure 3 shows that the leading-edge vortex has two modes at α =6°: the single vortex (Figure 3(a)) and the helical vortex (Figure 3(c)). The clear single vortex core parallel to the leading edge swings with a much small angle, which is not as steady as the leading-edge vortex of delta wings. Sometimes, the single vortex transforms to the helical vortex which has a sign consistent with the single vortex. Figures 3(b), (d) reveal that the vortex core rotates near the wing surface (Z'/S<4%) at X'/S≈20% on the sectional plane.

When the angle of attack increases to α =8°, the dual vortex structure emerges as shown in Figure 4. On the left forewing, the two leading-edge vortices with the same sign approach, twist with each other, and then separate. Afterward, the process starts again. In Figure 4(b), the inner vortex core close to the leading edge turns around in the range 15% <X'/S <20%, and the outer vortex core is in the range 30% <X'/S <35%. At α =8°, not only the vortex core is clearer than that at α =6°, but also the rotating sign and the core size are more distinguishable.

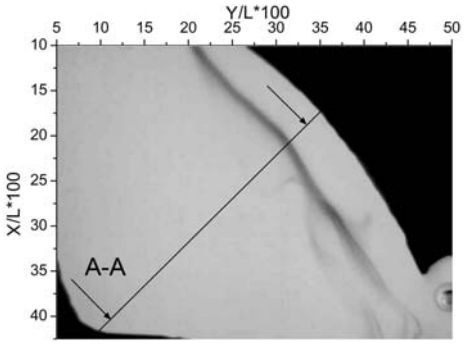

(a) top view of the single vortex

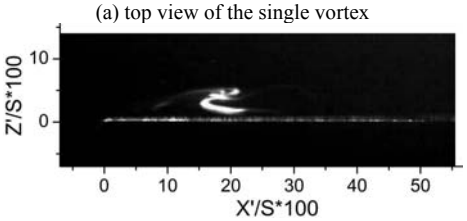

(b) A-A sectional view of the single vortex

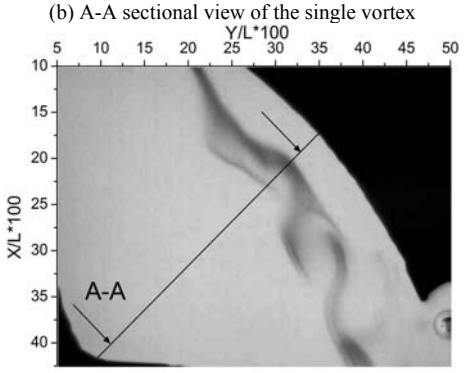

(c) top view of the helical vortex

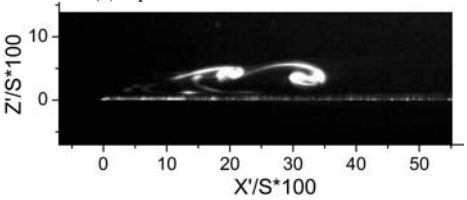

(d) A-A sectional view of the helical vortex

Figure 3: leading-edge vortex at α =6°

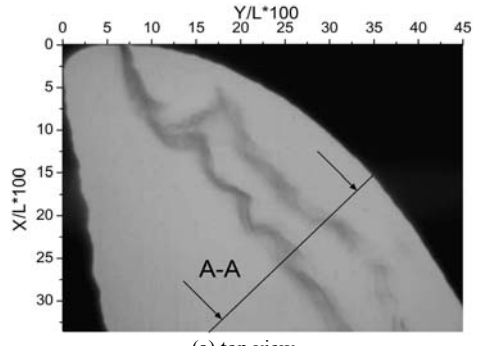

(a) top view

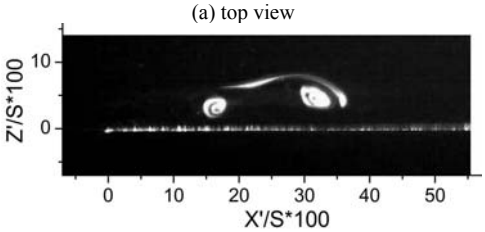

(b) A-A sectional view

Figure 4: leading-edge vortex at α =8°

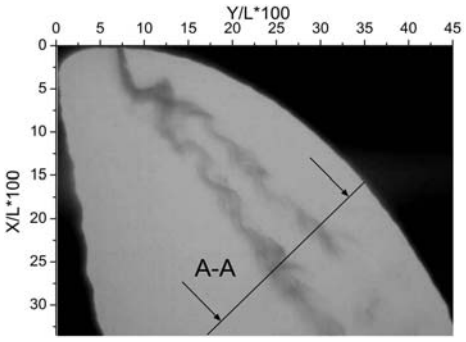

(a) top view

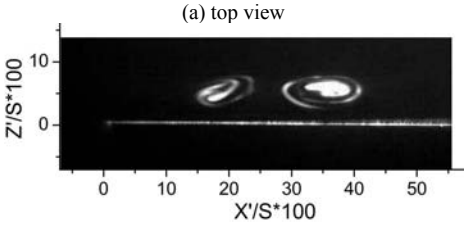

(b) A-A sectional view

Figure 5: leading-edge vortex at α =10°

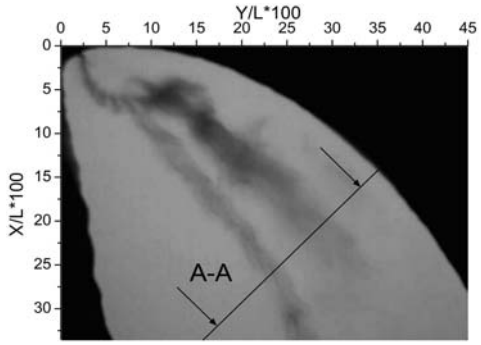

(a) top view

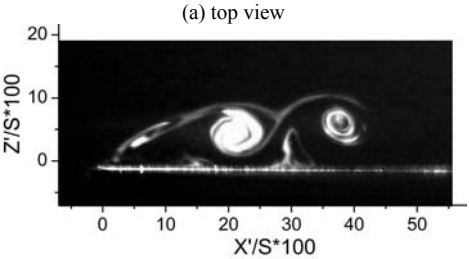

(b) A-A sectional view

Figure 6: leading-edge vortex at α =12°

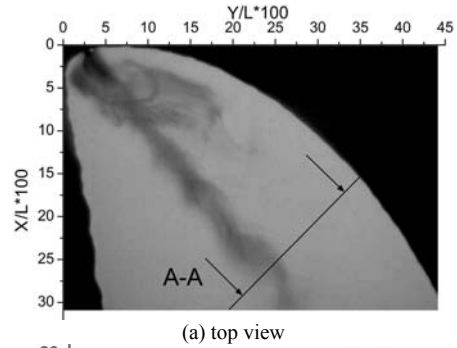

(a) top view

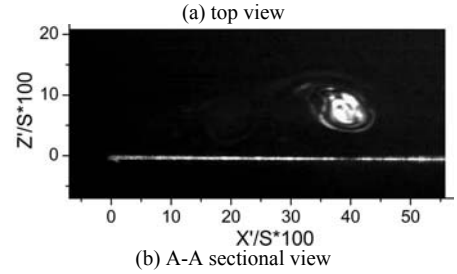

(b) A-A sectional view

Figure 7: leading-edge vortex at α =14°

The dual vortex structure is much steadier at α =10° and the two vortex cores no longer twist with each other. This indicates that the leading-edge vortices increase in both stability and strength with angle of attack. Albeit the sectional plane is not perpendicular absolutely to the cores of the dual vortex structure, it is clear that the two core diameters increase with angle of attack and the rotation speed of the inner vortex is slower than that of the outer vortex. As shown in Figure 5(b), the two vortex cores locate at X'/S=20% and 35% respectively, and the distance to the wing surface is Z'/S ≈ 5%. As the angle of attack increases, the dual vortex structure moves away from the surface and goes to the outboard of the model, simultaneously.

It can be seen from Figure 6(a) that there is a visible spiral point in the front of the wing at α =12° and the inner vortex decelerates. Figure 6(b) shows that both vortex cores become more diffusive and increase in size. Particularly, the core diameter of the inner vortex is almost twice that of the outer vortex. The vortex cores rotate at X'/S=20% and 40% respectively, and approach outboard of the wing even more. At this angle of attack, although the dual vortex structure is not as unsteady as the two leading-edge vortices twisting with each other on the left forewing at α =8°, the two vortices interacting on each other result in much complicated flow structure due to the increase in the two core diameters and the outer vortex strength.

At α =12°, the rotation speed of the inner vortex is slowed down, and its strength becomes weak. When the angle of attack increases to α =14°, the spiral point forms completely and the inner vortex disappears. There is only one leading-edge vortex extending from the spiral point on the left forewing, and the single vortex core rotates at X'/Z=40% in Figure 7.

The result of PIV measurements in the following section indicates that the axial velocity of the primary (outer) leading-edge vortex core is much less than the free stream velocity. This is different from the leading-edge vortex of delta wings of which the axial velocity can double or triple the free stream velocity [14]–[16]. The rotation speed and the core centralization of the leading-edge vortex for the butterfly model are weaker than that for delta wings. Therefore, the leading-edge vortex of the butterfly model is not as steady as that of delta wings. Not only the inner and outer vortex cores twist with each other at α =8°, but also the interaction of the two vortices gives rise to complicated flow structures at α =12°. Besides, it can be clearly seen from Figure 6(b) that the secondary vortex splits the leading-edge vortex into the dual vortex structure as observed by Taylor et al. [11] and Wang et al. [12], [13].

Chen et al. [17] reported the numerical simulation and the flow visualization for a 50° sweep delta wing. They suggested that the primary (inner) vortex of the dual vortex structure extends from the apex of the delta wing but the secondary (outer) vortex close to the leading edge flows round the primary vortex and forms downstream of the apex. Although the front extreme point of the butterfly model is not as sharp as the apex of the delta wings, it is the dual vortex structure of the butterfly model extending from the spiral point in the front of the wing and going along the leading edge that is akin to the dual vortex structure for the delta wing indicated by Chen et al [17].

3.2 Axial Velocity of Primary (Outer) Vortex Core

The dye visualization experiment indicated the existence of leading edge dual vortex structure at α =8°, 10° and 12°, respectively. The rotation speed of the inner vortex, close to the leading edge, is slower than that of the outer vortex and it vanishes at α =14°. It is obvious that the outer vortex is the primary vortex of the dual vortex structure for the butterfly model. Consequently, the PIV measurements are focused on the axial velocity of the primary (outer) vortex core.

Because the primary (outer) vortex swings with a small angle on the top view when the inner and outer vortices approach and twist with each other at some angles of attack, the laser sheet cuts through the middle of the primary leading-edge vortex core to obtain the PIV interrogation plane which has a angle with the wing surface of the butterfly model. In the flow field (Figure 8), the streamlines with arrowheads indicate the flow direction. There is a separation line and a confluence line in both flow fields. The separation line is the primary leading-edge vortex core. The confluence line is the cutting line of the leading edge shear layer by the PIV interrogation plane. A spiral point appears in the instantaneous flow field (Figure 8(a)) that shows more details, which can not be captured in the mean flow field (Figure 8(b)).

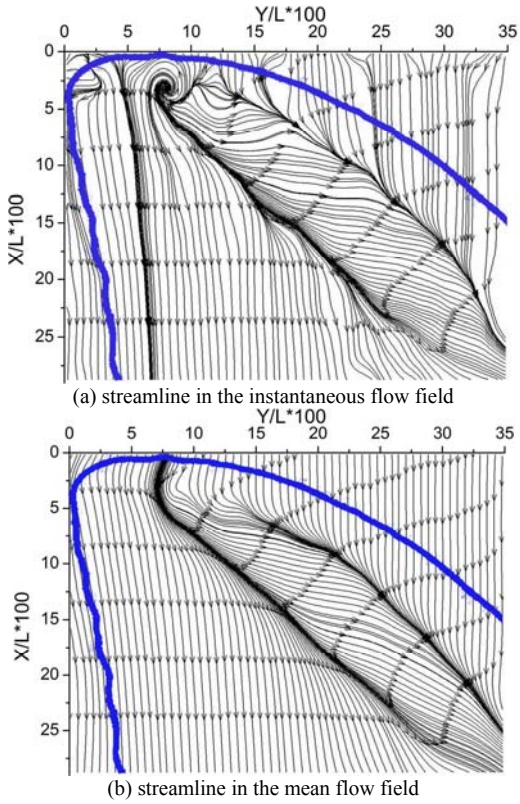

(a) streamline in the instantaneous flow field

(b) streamline in the mean flow field

Figure 8: streamline in flow field on the plane through the primary leading-edge vortex core (α =8°)
(the blue solid line is the outline of the butterfly model)

Although Figure 8 reveals the primary leading-edge vortex core clearly, the vortex axis coordinates and the velocity vectors of the points on the vortex axis must be extracted from the velocity field in order to investigate the axial velocity of the primary vortex core. Therefore, some spanwise horizontal lines are applied to cut the vortex core in

the range of 5%≤X/L≤25% with a step of 2.5%. Then the velocity vectors of the points on the spanwise horizontal line are decomposed orthogonally in the axial direction and the perpendicular direction of the primary vortex core. The point, which has the perpendicular velocity of zero, is on the primary leading-edge vortex axis. By the aforementioned method, the lines threading the vortex axis points for α =8° and α =12° are shown respectively in Figure 9. The vortex axes in the instantaneous and mean flow fields coincide well indicating that the method acquiring the primary vortex axis coordinates is feasible.

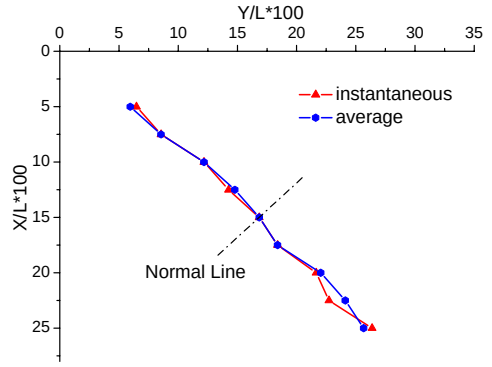

(a) α =8°

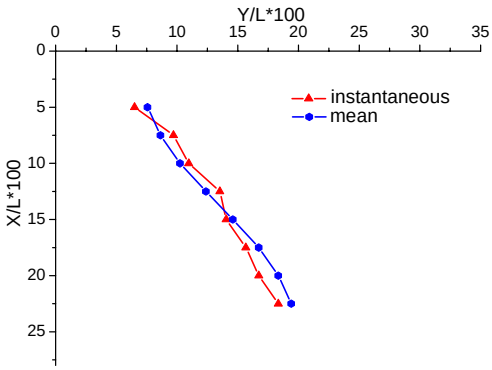

(b) α =12°

Figure 9: position of the primary leading-edge vortex axis

The axial velocity of the primary leading-edge vortex core in the streamwise direction is shown in Figure 10. In the mean flow fields, the axial velocity is less than the free stream velocity U in the range of 5%≤X/L≤25% at α =8° and α =12°. Along the primary leading-edge vortex to the downstream, the axial velocity normalized by the free stream velocity increases to a lower extreme value U_{core}/U≈30%, and after a slight decrease it rises again. Figure 11 shows that the turbulence intensity of the axial velocity has different variation trends for α =8° and α =12°. At α =8°, the turbulence intensity decreases in the streamwise direction, but that is opposite at α =12°.

In order to further examine the axial velocity, a line normal to the primary leading-edge vortex axis is inserted (as the dashed line in Figure 9(a)) and velocity vectors of the points on the normal line are decomposed orthogonally in the axial direction and the perpendicular direction. When the axial velocity of the vortex core is larger than that of the both side flow, we will call it a "jet-like" axial velocity profile. The opposite is a "wake-like" profile. That is in concordance with the delta wings literatures [15], [16]. Figure 12 is the axial velocity profile across the point on the primary vortex axis at X/L=15% for α =8°. The point, of which the perpendicular velocity is zero, is on the primary leading-edge vortex axis and its axial velocity is larger than that of the both sides (as shown in the dashed ellipse of Figure 12), so it is a "jet-like" axial velocity profile.

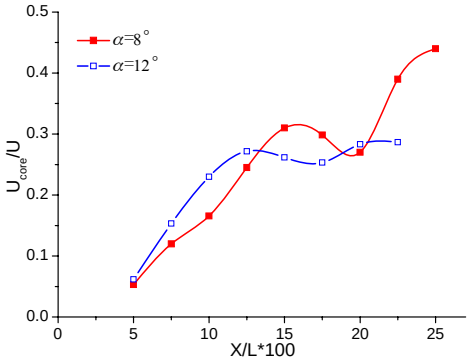

Figure 10: axial velocity of the primary leading-edge vortex core in the mean flow field

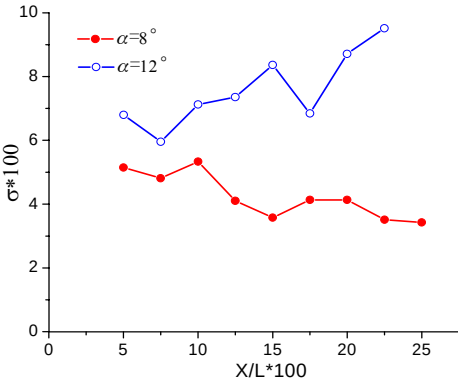

Figure 11: turbulence intensity of the axial velocity

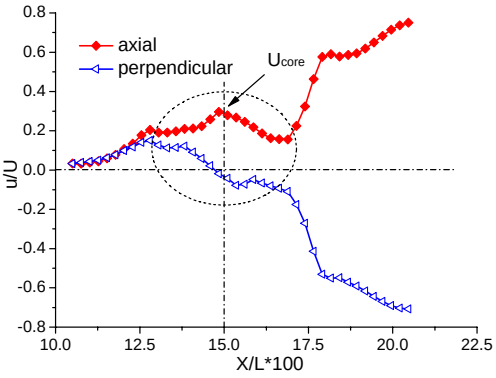

(a) instantaneous flow field

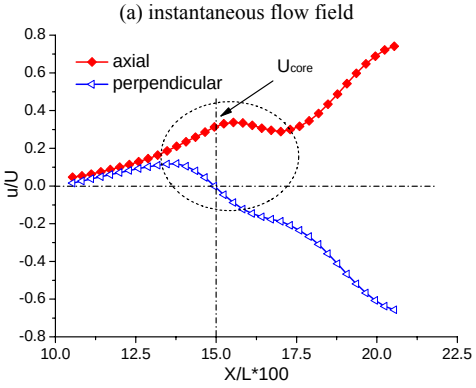

(b) mean flow field

Figure 12: axial velocity profile of the primary leading-edge vortex core (α =8°，X/L=15%)

Table 1 shows the different axial velocity profile types observed at α =8° and α =12°. At α =8°, the slow axial

velocity near the front of the model is so difficult to be distinguished from the local velocity that the classification is ambiguous, for example in the range 5%≤X/L≤10%. But at X/L=12.5%, the axial velocity of the primary vortex core is smaller than that of the both sides so it reveals a "wake-like" axial velocity profile. The transition from a "wake-like" to a "jet-like" profile occurs at X/L≈15% (as shown in Figure 12), while the axial velocity reaches its lower extreme value U_{core}/U≈30% (see Figure 10). When the angle of attack is α =12°, the axial velocity profile variation is similar to that at α =8°. Yet, the switch point from a "wake-like" to a "jet-like" profile is obtained at X/L≈12.5% which is smaller than that for α =8° at X/L≈15%.

	α =8°	α =12°
X/L=5%	-	-
X/L=7.5%	-	wake-like
X/L=10%	-	wake-like
X/L=12.5%	wake-like	jet-like
X/L=15%	jet-like	jet-like
X/L=17.5%	jet-like	jet-like
X/L=20%	jet-like	jet-like
X/L=22.5%	jet-like	jet-like
X/L=25%	jet-like	jet-like

Table 1: axial velocity profile
("-" means an ambiguous axial velocity profile)

4 CONCLUSION

The dye visualizations and the Particle Image Velocimetry (PIV) measurements have been conducted to investigate the flow structure and the axial velocity of the primary vortex core for the leading-edge vortex of the simplified butterfly model. The main conclusions obtained from this work are outlined in the following.

In the dye visualization experiment, it is observed that there exists the leading edge dual vortex structure at some angles of attack for the butterfly model as that for low Reynolds number flow over non-slender delta wings. This structure is formed due to the secondary vortex which splits the leading-edge vortex downstream of the model apex. Therefore, the dual vortex structure is a common structure for low Reynolds number flow over wings. As the angle of attack increases, the dual vortex structure approaches outboard of the wing and the core diameter increases.

The PIV measurement results indicate that the axial velocity of the primary (outer) leading-edge vortex core increases to the lower extreme value, and after a slight decrease it rises again in the streamwise direction. When the transition from a "wake-like" to a "jet-like" axial velocity profile occurs, the axial velocity reaches to the lower extreme value. In addition, the turbulence intensity of the axial velocity presents opposite trends at α =8° and α =12°.

ACKNOWLEDGMENT

This work is supported by National Natural Science Foundation of China (NSFC) under grant no. 10425207.

REFERENCES

[1]S. P. Sane, and M. H. Dickinson. The aerodynamic effects of wing rotation and a revised quasi-steady model of flapping flight. *The Journal of Experimental Biology*, 205(8): 1087–1096, 2002.

[2]R. Zbikowski. On aerodynamic modeling of an insect–like flapping wing in hover for Micro Air Vehicles. *Philosophical Transactions A of the Royal Society*, 360(1791): 273–290, 2002.

[3] J. H. Backenbury. Kinematics of take–off and climbing fight in butterflies. *Journal of Zoological of London*, 244: 251–270, 1991.

[4]C. R. Betts, and R. J. Wootton. Wing shape and fight behavior in butterflies (Lepidoptera: *Papilionoidea* and *Hesperioidea*): a preliminary analysis. *The Journal of Experimental Biology*, 138: 271–288, 1988.

[5]R. Dudley. Biomechanics of flight in neotropical butterflies: morphometrics and kinematics. *The Journal of Experimental Biology*, 150: 37–53, 1990.

[6]R. B. Srygley, and A. L. R. Thomas. Unconventional lift–generating mechanisms in free–flying butterflies. *Nature*, 420(6916): 660–664, 2002.

[7]S. Kei, S. Masakazu, and S. Takanori. Study on flapping–of–wings flight of butterfly with experimental measurement. AIAA Atmospheric Flight Mechanics Conference, Providence, Rhode Island, AIAA 2004–5368, Aug. 2004.

[8]Y. Hu, J. J. Wang, P. F. Zhang, and C. Zhang. Experimental investigation on the flow structure over a simplified *Papilio ulysses* model. *Chinese Science Bulletin*, 54(6): 1026–1031, 2009.

[9]Y. Hu, J. J. Wang, C. Zhang, and P. F. Zhang. Shape of a butterfly wing affects flow structures. *Acta Aerodynamica Sinica*, 2008, accepted to appear (in Chinese).

[10]Y. Hu, and J. J. Wang. Experimental investigation on the aerodynamic performance of gliding butterflies. Submitted to AIAA Journal.

[11]G. S. Taylor, T. Schnorbus, and I. Gursul. An investigation of vortex flows over low sweep delta wings. 33rd AIAA Fluid Dynamics Conference, Orlando, Florida, AIAA 2003–4021, June 2003.

[12]J. J. Wang, and W. Zhang. Experimental investigations on leading–edge vortex structures for flow over non–slender delta wings," *Chinese Physical Letters*, 25(7): 2550–2553, 2008.

[13]J. J. Wang, X. Zhao, W. C. Liu, and J. Q. Tu. Experimental investigation on flow structures over nonslender delta wings at low reynolds numbers. *Journal of Experiments in Fluid Mechanics*, 21(2): 1–7, 2007.

[14]J. J. Wang, F. Y. Miao, Z. N. Niu, and Q. Z. Xue. The effects of trailing edge jets on the vortex breakdown of a delta wing. *Acta Aerodynamica Sinica*, 18(2): 125–131, 2000 (in Chinese).

[15] R. Gordnier, M. Visbal. Higher–order compact difference scheme applied to the simulation of a low sweep delta wing flow. 41st Aerospace Sciences Meeting, Reno, Nevada, AIAA 2003–620, Jan. 2003.

[16]V. OL. Michael., Leading–edge vortex structure of nonslender delta wings at low reynolds number. *AIAA Journal*, 41(1): 16–26, 2003.

[17]L. Chen, J. J. Wang, L. X. Zuo, and L. H. Feng. Vortex flows over 50° swept delta wing at low reynolds number. *Acta Aerodynamica Sinica*, 2009, acceptedto appear (in Chinese).